Update on J/ψ regeneration in a hadron gas

L. M. Abreu[*]
Instituto de Física, Universidade Federal da Bahia, Campus Universitário de Ondina, 40170-115, Bahia, Brazil

K. P. Khemchandani[†]
Universidade Federal de São Paulo, 01302-907, São Paulo, Brazil

A. Martínez Torres[‡]
Instituto de Física, Universidade de São Paulo, Rua do Matão 1371, 05508-090 São Paulo, São Paulo, Brazil

F. S. Navarra[§]
Instituto de Física, Universidade de São Paulo, Rua do Matão 1371, 05508-090 São Paulo, São Paulo, Brazil and Institut de Physique Théorique, Université Paris Saclay, CEA, CNRS, F-91191, Gif-sur-Yvette, France

M. Nielsen[‖]
Instituto de Física, Universidade de São Paulo, Rua do Matão 1371, 05508-090 São Paulo, São Paulo, Brazil and SLAC Nacional Acelerator Laboratory, Stanford University, Stanford, California 94309, USA

(Received 25 December 2017; revised manuscript received 28 February 2018; published 5 April 2018)

In heavy-ion collisions, after the quark-gluon plasma there is a hadronic gas phase. Using effective Lagrangians, we study the interactions of charmed mesons which lead to J/ψ production and absorption in this gas. We update and extend previous calculations introducing strange meson interactions and also including the interactions mediated by the recently measured exotic charmonium resonances $Z(3900)$ and $Z(4025)$. These resonances open new reaction channels for the J/ψ, which could potentially lead to changes in its multiplicity. We compute the J/ψ production cross section in processes such as $D_{(s)}^{(*)} + \bar{D}^{(*)} \to J/\psi + (\pi, \rho, K, K^*)$ and also the J/ψ absorption cross section in the corresponding inverse processes. Using the obtained cross sections as input to solve the appropriate rate equation, we conclude that the interactions in the hadron gas phase lead to a 20–24% reduction of the J/ψ abundance. Within the uncertainties of the calculation, this reduction is the same at the Relativistic Heavy Ion Collider and the large Hadron Collider.

DOI: 10.1103/PhysRevC.97.044902

I. INTRODUCTION

Precise measurements of the J/ψ multiplicity in heavy-ion collisions are an important source of information about the properties of the quark-gluon plasma phase (QGP) [1]. During this phase, J/ψ's are destroyed and created in a complex and rich dynamical process, which involves many properties of the QGP which we wish to know better. After cooling and hadronization, there is a hadron gas phase, which may distort or even completely wash out the information carried by the J/ψ's about the hot QGP phase. Much work has been devoted to understand the interactions of the J/ψ in a hadron gas and the most important process, i.e., the $J/\psi - \pi$ reaction (and the inverse process), has been exhaustively studied in many papers [2–10]. The results of these different calculations eventually converged and today we can say that the $J/\psi - \pi$ cross section is known with reasonable precision. The J/ψ interactions have already been investigated with field theory models [2–5], quark models [6], QCD sum rules [7], and other approaches [8–10]. Most of these papers are more than ten years old and they focus on J/ψ suppression, which had been considered a signature of the quark-gluon plasma. However, in the past decade experimental data have shown that at the CERN Super Proton Synchrotron (SPS) and at the Relativistic Heavy Ion Collider (RHIC) nearly the same amount of J/ψ suppression is observed. More recently, after the observation of an "unsuppression" at the Large Hadron Collider (LHC), the focus started to be the confirmation of the enhancement of the J/ψ yield, which became one of the new signatures of the QGP dynamics.

[*]luciano.abreu@ufba.br
[†]kanchan@if.usp.br
[‡]amartine@if.usp.br
[§]navarra@if.usp.br
[‖]mnielsen@if.usp.br

After pions, kaons are the next lightest and also very abundant mesons in a hadron gas. PHENIX data on particle production in Au-Au collisions [11] show that at low transverse momentum ($p_T \simeq 0.5$–1.5 GeV) the ratio $(K^+ + K^-)/(\pi^+ + \pi^-)$ goes to the value 0.50. Recent ALICE data on particle production in Pb-Pb collisions [12] in a similar p_T range show that this ratio is close to 0.45. Particles with these values of p_T most certainly come from the hadron gas. Taking into account the neutral states, kaons may be up to 30% of all mesons in the hadron gas. Curiously, there are few works addressing the $J/\psi - K$ interaction [13] and even fewer works addressing the $J/\psi - K^*$ interaction [14]. This lack of knowledge and the potential changes in the final J/ψ abundance that kaons and other strange mesons might cause justifies the efforts to improve the existing calculations of the J/ψ, strange meson dissociation cross sections and also the inverse reactions. Indeed, in his opening talk at 2017 Quark Matter Conference [15], Schukraft formulated a list of goals to be achieved by the heavy-ion physics community in the near future. One of them is to understand processes such as $D + \bar{D} \to J/\psi + X$ and $D_s + \bar{D} \to J/\psi + X$, which happen during the late hadronic phase of heavy-ion collisions and increase the number of J/ψ's. These processes are said to yield "J/ψ regeneration" [16,17] and they are background for J/ψ production by recombination of charm-anticharm pairs during the plasma phase.

Further motivation to revisit the study of J/ψ interactions with light mesons comes from the striking experimental information which appeared after the first round of studies of J/ψ interactions (roughly from 1995 to 2005): the existence of new charmonium states, the so-called X, Y, and Z states, which started to be observed in 2003 [18]. Some of these states generate new channels for the J/ψ-light meson reactions and could potentially change the cross sections. We investigate the subject by computing the cross sections of processes involving $Z_c(3900)$ and $Z_c(4025)$.

In this work, we study J/ψ production in reactions involving pions and strange mesons, such as $D^{(*)} + \bar{D}^{(*)} \to J/\psi + \pi$, $D^{(*)} + \bar{D}^{(*)} \to J/\psi + \rho$, $D_s^{(*)} + \bar{D}^{(*)} \to J/\psi + K$, and $D_s^{(*)} + \bar{D}^{(*)} \to J/\psi + K^*$. As was pointed out in Ref. [10] (see Fig. 20 of that work), the reactions initiated by D's and D_s's have the same order of magnitude. Making use of the effective Lagrangians discussed in Refs. [3,5,13,14], we will obtain the cross sections for the above-mentioned processes and with them we determine the thermally averaged cross sections for dissociation and production reactions. These latter are then used as input in rate equations, which can be solved, giving the J/ψ abundance in heavy-ion collisions. In some works (see, for example, Refs. [4,19–21]), on the J/ψ dissociation in a hadron gas, medium effects are explicitly included. We are not going to take these effects into account, since in our formalism the J/ψ interactions are already treated individually and the use of medium modifications (such as, e.g., in-medium masses) might lead to a double counting of the interactions. Also, we are not going to include in the calculation the J/ψ's which result from the radiative decays of the $\psi(2S)$'s.

The paper is organized as follows. In Sec. II, we describe the formalism and determine the production and absorption cross sections for $\pi J/\psi$, $\rho J/\psi$, and $K^{(*)} J/\psi$ reactions. Then, in Sec. III, we present and discuss the results obtained for thermally averaged cross sections. After that, Sec. IV is devoted to the analysis of J/ψ abundance in heavy-ion collisions. Finally, in Sec. V we draw the concluding remarks.

II. INTERACTIONS BETWEEN J/ψ AND LIGHT MESONS

Our starting point is the calculation of the cross sections for the $\varphi - J/\psi$ interactions, where φ denotes a pseudoscalar or vector meson. To this end, we follow Refs. [3,5,13,14] and use the effective couplings between pseudoscalar and vector mesons within the framework of an SU(4) effective theory. This is an effective formalism in which the vector mesons are identified as the gauge bosons, and the relevant Lagrangians are given by [3,4]

$$\begin{aligned}
\mathcal{L}_{PPV} &= -ig_{PPV}\langle V^\mu [P, \partial_\mu P]\rangle, \\
\mathcal{L}_{VVV} &= ig_{VVV}\langle \partial_\mu V_\nu [V^\mu, V^\nu]\rangle, \\
\mathcal{L}_{PPVV} &= g_{PPVV}\langle PV^\mu [V_\mu, P]\rangle, \\
\mathcal{L}_{VVVV} &= g_{VVVV}\langle V^\mu V^\nu [V_\mu, V_\nu]\rangle,
\end{aligned} \tag{1}$$

where the indices PPV, VVV, $PPVV$, and $VVVV$ denote the type of vertex incorporating pseudoscalar and vector meson fields in the couplings [3,4,13,14] and g_{PPV}, g_{VVV}, g_{PPVV}, and g_{VVVV} are the respective coupling constants. The symbol $\langle \cdots \rangle$ stands for the trace over SU(4) matrices and V_μ represents a SU(4) matrix. In the derivation of the SU(4) theory of meson interactions, one works first with mathematical states. The physical states are combinations of the mathematical states. Usually one assumes what is called "ideal mixing," which means that the physical states are just described by their most important components. Here we follow Ref. [22], where V_μ is parametrized by 16 vector-meson fields including the 15-plet and singlet of SU(4),

$$V_\mu = \begin{pmatrix} \frac{\omega}{\sqrt{2}} + \frac{\rho^0}{\sqrt{2}} & \rho^+ & K^{*+} & \bar{D}^{*0} \\ \rho^- & \frac{\omega}{\sqrt{2}} - \frac{\rho^0}{\sqrt{2}} & K^{*0} & D^{*-} \\ K^{*-} & \bar{K}^{*0} & \phi & D_s^{*-} \\ D^{*0} & D^{*+} & D_s^{*+} & J/\psi \end{pmatrix}_\mu ; \tag{2}$$

and P is a matrix containing the 15-plet of the pseudoscalar meson fields, written in the physical basis in which η, η' mixing is taken into account,

$$P = \begin{pmatrix} \frac{\eta}{\sqrt{3}} + \frac{\eta'}{\sqrt{6}} + \frac{\pi^0}{\sqrt{2}} & \pi^+ & K^+ & \bar{D}^0 \\ \pi^- & \frac{\eta}{\sqrt{3}} + \frac{\eta'}{\sqrt{6}} - \frac{\pi^0}{\sqrt{2}} & K^0 & D^- \\ K^- & \bar{K}^0 & -\frac{\eta}{\sqrt{3}} + \sqrt{\frac{2}{3}}\eta' & D_s^- \\ D^0 & D^+ & D_s^+ & \eta_c \end{pmatrix}. \tag{3}$$

In addition to the terms given above, we also consider anomalous parity terms. The anomalous parity interactions with vector fields can be described in terms of the gauged Wess-Zumino action [3], which can be summarized as

$$\begin{aligned}
\mathcal{L}_{PVV} &= -g_{PVV}\varepsilon^{\mu\nu\alpha\beta}\langle \partial_\mu V_\nu \partial_\alpha V_\beta P\rangle, \\
\mathcal{L}_{PPPV} &= -ig_{PPPV}\varepsilon^{\mu\nu\alpha\beta}\langle V_\mu (\partial_\nu P)(\partial_\alpha P)(\partial_\beta P)\rangle, \\
\mathcal{L}_{PVVV} &= ig_{PVVV}\varepsilon^{\mu\nu\alpha\beta}\big[\langle V_\mu V_\nu V_\alpha \partial_\beta P\rangle
\end{aligned}$$

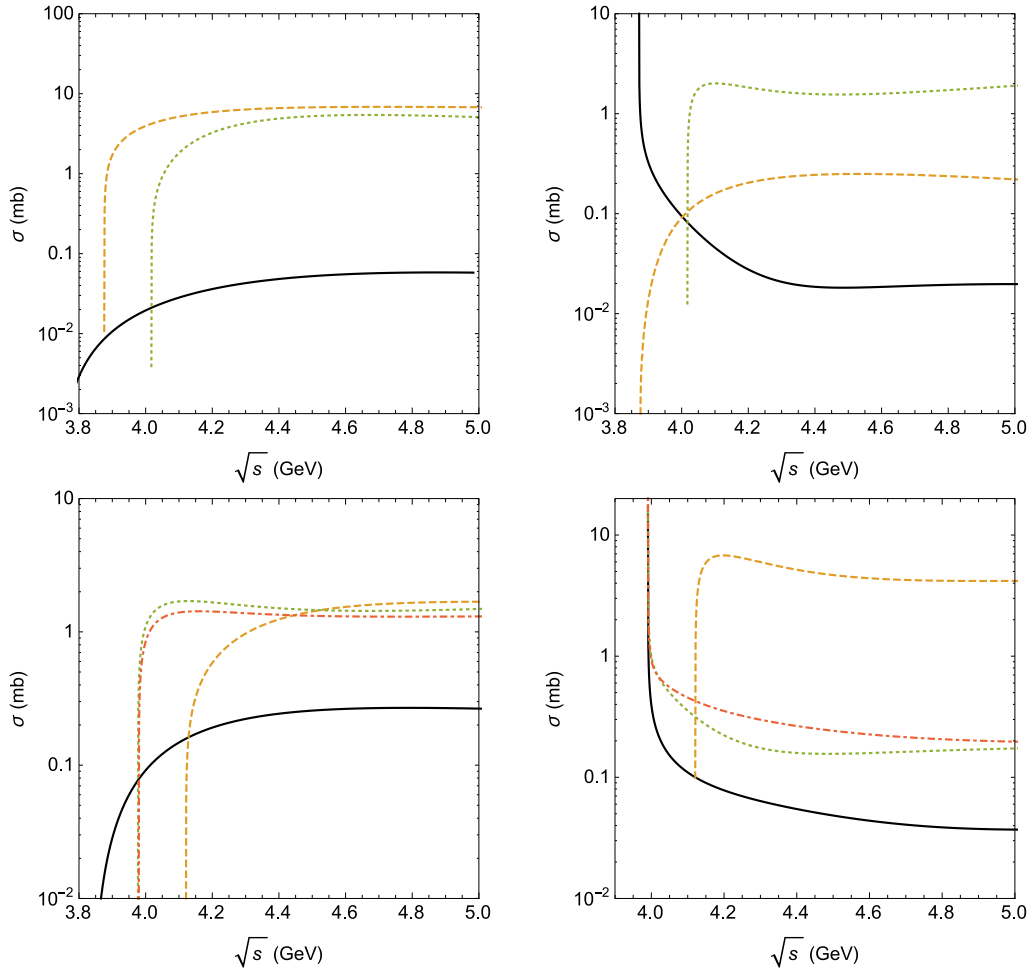

FIG. 1. J/ψ absorption cross sections in different processes as a function of the c.m. energy $\sqrt{s}$. Top left panel: $\pi J/\psi$ in the initial state. Top right panel: $\rho J/\psi$ in the initial state. Solid, dashed, and dotted lines represent the $\pi(\rho)J/\psi \to D\bar{D}$, $\pi(\rho)J/\psi \to D^*\bar{D}$, and $\pi(\rho)J/\psi \to D^*\bar{D}^*$ reactions, respectively. Bottom left panel: KJ/ψ in the initial state. Bottom right panel: K^*J/ψ in the initial state. Solid, dashed, dotted, and dot-dashed lines represent the $K^{(*)}J/\psi \to D_s\bar{D}$, $K^{(*)}J/\psi \to D_s^*\bar{D}^*$, $K^{(*)}J/\psi \to D_s^*\bar{D}$, and $K^{(*)}J/\psi \to D_s\bar{D}^*$ reactions, respectively.

$$+\tfrac{1}{3}\langle V_\mu(\partial_\nu V_\alpha)V_\beta P\rangle\Big]. \tag{4}$$

The g_{PVV}, g_{PPPV}, and g_{PVVV} are the coupling constants of the PVV, $PPPV$, and $PVVV$ vertices, respectively [3–5,13,14]. The couplings given by the effective Lagrangians in Eqs. (1) and (4) allow us to study the following $\varphi J/\psi$ absorption processes:

$$\begin{aligned}
&(1)\ \varphi J/\psi \to D_{(s)}\bar{D},\\
&(2)\ \varphi J/\psi \to D^*_{(s)}\bar{D}^*,\\
&(3)\ \varphi J/\psi \to D^*_{(s)}\bar{D},\\
&(4)\ \varphi J/\psi \to D_{(s)}\bar{D}^*,
\end{aligned} \tag{5}$$

where the final states with strange charmed mesons stand for the initial states with K and K^* mesons, while final states with unflavored charmed mesons appear for the initial states with pions and ρ mesons. In the present approach, the diagrams considered to compute the amplitudes of the processes above are of two types: one-meson exchange and contact graphs. They are shown in Fig. 1 of Refs. [3,13,14] for the reactions involving π, K, and K^*, respectively, and in Fig. 2 of Ref. [3] for those with ρ.

We define the invariant amplitudes for the processes (1)–(4) in Eq. (5) involving $\varphi = \pi, K$ mesons as

$$\begin{aligned}
\mathcal{M}_1^{(\varphi)} &= \sum_i \mathcal{M}_{1i}^{(\varphi)\mu}\epsilon_\mu(p_2),\\
\mathcal{M}_2^{(\varphi)} &= \sum_i \mathcal{M}_{2i}^{(\varphi)\mu\nu\lambda}\epsilon_\mu(p_2)\epsilon_\nu^*(p_3)\epsilon_\lambda^*(p_4),\\
\mathcal{M}_3^{(\varphi)} &= \sum_i \mathcal{M}_{3i}^{(\varphi)\mu\nu}\epsilon_\mu(p_2)\epsilon_\nu^*(p_3),\\
\mathcal{M}_4^{(\varphi)} &= \sum_i \mathcal{M}_{4i}^{(\varphi)\mu\nu}\epsilon_\mu(p_2)\epsilon_\nu^*(p_4).
\end{aligned} \tag{6}$$

In the above equations, the sum over i represents the sum over all diagrams contributing to the respective amplitude; p_j denotes the momentum of particle j, with particles 1 and 2 standing for initial state mesons, and particles 3 and 4 for final-state mesons; $\epsilon_\mu(p_j)$ is the polarization vector related

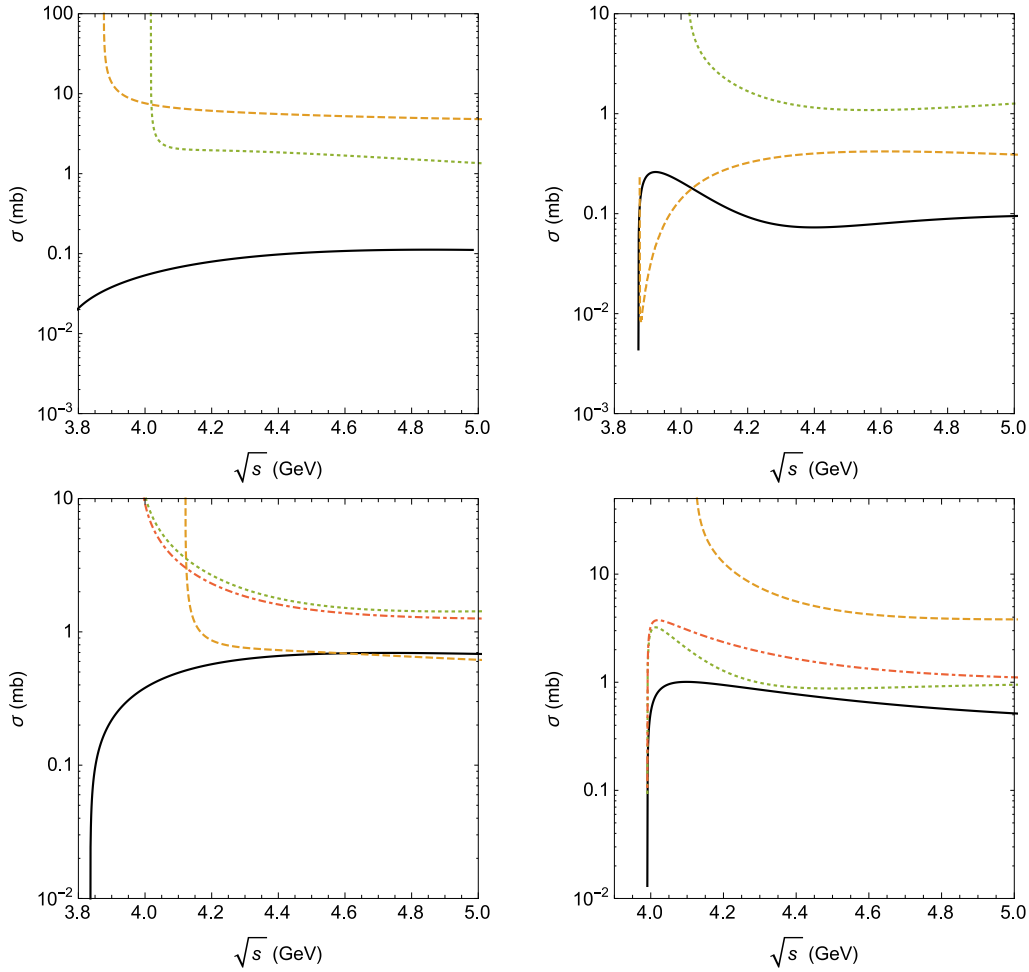

FIG. 2. J/Ψ production cross sections in different processes as a function of the c.m. energy $\sqrt{s}$. Top left panel: $\pi J/\psi$ in the final state. Top right panel: $\rho J/\psi$ in the final state. Solid, dashed, and dotted lines represent the $D\bar{D} \to \pi(\rho)J/\psi$, $D^*\bar{D} \to \pi(\rho)J/\psi$, and $D^*\bar{D}^* \to \pi(\rho)J/\psi$ reactions, respectively. Bottom left panel: KJ/ψ in the final state. Bottom right panel: K^*J/ψ in the final state. Solid, dashed, dotted, and dot-dashed lines represent the $D_s\bar{D} \to K^{(*)}J/\psi$, $D_s^*\bar{D}^* \to K^{(*)}J/\psi$, $D_s^*\bar{D} \to K^{(*)}J/\psi$, and $D_s\bar{D}^* \to K^{(*)}J/\psi$ reactions, respectively.

to the respective vector particle j. The explicit expressions of amplitudes $\mathcal{M}^{(\pi)}$ and $\mathcal{M}^{(K)}$ we use in the present work are reported in Refs. [3,13], respectively.

In the case of processes involving $\varphi = \rho, K^*$ mesons, we must add on the right-hand side of each expression in Eq. (6) the contraction of the amplitude with the polarization vector of vector meson, i.e., for the reaction (1) we have $\mathcal{M}_1^{(\varphi)\mu\nu}\epsilon_\mu(p_1)\epsilon_\nu(p_2)$ and so on. The explicit expressions of the amplitudes $\mathcal{M}^{(\rho)}$ and $\mathcal{M}^{(K^*)}$ used here are those published in Refs. [3,13,14], with some minor changes [23].

We are interested in the determination of the isospin-spin-averaged cross section for the processes in Eq. (5), which in the center of mass (c.m.) frame is defined as

$$\sigma_r^{(\varphi)}(s) = \frac{1}{64\pi^2 s}\frac{|\vec{p}_f|}{|\vec{p}_i|}\int d\Omega \overline{\sum_{S,I}}\left|\mathcal{M}_r^{(\varphi)}(s,\theta)\right|^2, \tag{7}$$

where $r = 1,2,3,4$ labels $\varphi - J/\psi$ absorption processes according to Eq. (6); $\sqrt{s}$ is the c.m. energy; $|\vec{p}_i|$ and $|\vec{p}_f|$ denote the three-momenta of initial and final particles in the c.m. frame, respectively; and the symbol $\overline{\sum_{S,I}}$ represents the sum over the spins and isospins of the particles in the initial and final states, weighted by the isospin and spin degeneracy factors of the two particles forming the initial state for the reaction r, i.e.,

$$\overline{\sum_{S,I}}|\mathcal{M}_r|^2 = \frac{1}{g_1 g_2}\sum_{S,I}|\mathcal{M}_r|^2, \tag{8}$$

with $g_1 = (2I_{1i,r}+1)(2S_{1i,r}+1), g_2 = (2I_{2i,r}+1)(2S_{2i,r}+1)$ being the degeneracy factors of the initial particles 1 and 2.

We have employed in the computations of the present work the isospin-averaged masses: $m_\pi = 138.1$ MeV, $m_\rho = 775.2$ MeV, $m_K = 495.6$ MeV, $m_{K^*} = 893.7$ MeV, $m_D = 1867.2$ MeV, $m_{D^*} = 2008.6$ MeV, $m_{D_s} = 1968.3$ MeV, $m_{D_s^*} = 2112.1$ MeV, and $m_{J/\psi} = 3096.9$ MeV. Besides, the values of coupling constants appearing in the expressions of the amplitudes have been taken from Ref. [5] for $\mathcal{M}^{(\pi)}$; from Refs. [13,14] for $\mathcal{M}^{(K)}$ and $\mathcal{M}^{(K^*)}$; and from Ref. [3] for the couplings involving ρ meson in $\mathcal{M}^{(\rho)}$. We have also included form factors in the vertices when evaluating the cross sections.

They were taken from [3] and are

$$F_3 = \frac{\Lambda^2}{\Lambda^2 + \mathbf{q}^2}; \quad F_4 = \frac{\Lambda^2}{\Lambda^2 + \bar{\mathbf{q}}^2}\frac{\Lambda^2}{\Lambda^2 + \bar{\mathbf{q}}^2}, \tag{9}$$

where F_3 and F_4 are the form factor for the three-point and four-point vertices, respectively; $\mathbf{q} = (\mathbf{p_1} - \mathbf{p_3})^2$ or $(\mathbf{p_2} - \mathbf{p_3})^2$ for a vertex involving a t- or u-channel meson exchange; and $\bar{\mathbf{q}} = [(\mathbf{p_1} - \mathbf{p_3})^2 + (\mathbf{p_2} - \mathbf{p_3})^2]/2$. The cutoff parameter Λ was chosen to be $\Lambda = 2.0$ GeV for all vertices [3].

A. J/ψ absorption

On the top left panel of Fig. 1, the $\pi J/\psi$ absorption cross sections for the $\pi J/\psi \to D\bar{D}, D^*\bar{D}$, and $D^*\bar{D}^*$ reactions are plotted as a function of the c.m. energy $\sqrt{s}$. Both the magnitude and the relative importance of each of these reactions are in agreement with previous calculations based on QCD sum rules [7]. The cross sections of the processes $\rho J/\psi \to D\bar{D}, D^*\bar{D}^*$, and $D^*\bar{D}^*$ reactions are plotted as a function of $\sqrt{s}$ on the top right panel of the figure. We see that these cross sections have the same order of magnitude as those initiated by pions. This is also in agreement with other previous calculations (see, for example, Ref. [10]). On the bottom left panel of Fig. 1, the cross sections of the processes $K J/\psi \to D_s\bar{D}, D_s^*\bar{D}^*, D_s^*\bar{D}$, and $D_s\bar{D}^*$ reactions are shown. Finally, on the bottom right panel of the same figure, we show the cross sections of the processes initiated by K^*: $K^* J/\psi \to D_s\bar{D}, D_s^*\bar{D}^*, D_s^*\bar{D}$, and $D_s\bar{D}^*$. Both the magnitude and the relative importance of each of these reactions are in agreement with the results obtained in Ref. [10] and also with those obtained in Refs. [13] and [14]. There are some small differences due to different choices in the form factors and cutoff values. The most striking difference is in the strength of the K^* initiated processes, which in our case is remarkably larger.

Summarizing, despite the different $\sqrt{s}$ dependence of the $(\pi, \rho, K, K^*) - J/\psi$ absorption cross sections discussed above, their contributions can be considered to be approximately of the same order of magnitude, justifying the inclusion of all these contributions in the analysis of J/ψ abundance that will be done in next sections.

B. J/ψ production

We now calculate the cross sections of the inverse processes, which can be obtained from the direct processes through the use of detailed balance (see Eq. (48) from Ref. [5]). In the top left panel of Fig. 2, the $\pi J/\psi$ production cross sections for the $D\bar{D} \to \pi J/\psi, D^*\bar{D}^* \to \pi J/\psi$, and $D^*\bar{D} \to \pi J/\psi$ reactions are plotted as a function of the c.m. energy $\sqrt{s}$. In the top right panel of Fig. 2, the $\rho J/\psi$ production cross sections for the $D\bar{D} \to \rho J/\psi, D^*\bar{D}^* \to \rho J/\psi$, and $D^*\bar{D} \to \rho J/\psi$ reactions are plotted as a function of the c.m. energy $\sqrt{s}$. In the bottom left panel of Fig. 2, the $K J/\psi$ production cross sections are plotted, and in the bottom right panel of the same figure, the $K^* J/\psi$ production cross sections are plotted.

From these many curves, two general conclusions may be drawn: (i) Reactions which start or end with $\pi J/\Psi$ and $K^* J/\Psi$ have larger cross sections. (ii) Excluding the low-energy region (which will be much less relevant for phenomenology), the J/ψ production and absorption cross sections are very close to each other in almost all channels. Since the J/Ψ absorption and production cross sections have comparable magnitudes, what will determine the final yield of J/Ψ's will be the thermally averaged cross sections, which, reflecting the physical aspects of the hadron gas, will select the range of energies (in the horizontal axis of Figs. 1 and 2) which are more important.

C. The impact of the $Z(3900)$ and $Z(4025)$ resonances on J/ψ production

Over the past decade, the existence of exotic charmonium states has been well established. These are new states which contain a $c\bar{c}$ pair but are not conventional quark-antiquark configurations, being rather multiquark states. For the present work, some states are particularly relevant: those which decay into $J/\psi - \pi$, as the $Z_c(3900)$, and those which decay into $J/\psi - \rho$, as the $Z_c(4025)$. Indeed, these states open new s channels for J/ψ interactions, as, for example, $J/\psi + \pi \to Z_c \to D + \bar{D}^*$. These processes can change the results found in the previous section and hence deserve special attention. The impact of the best known of the exotic states, the $X(3872)$, on J/ψ interactions with light mesons was first investigated in Ref. [24], where the cross section of the reaction $J/\psi + \rho \to D + \bar{D}^*$ was calculated. The obtained cross section was very small and can then be neglected. More recently, the BES Collaboration observed [25] and then confirmed [26] the $Z_c^{\pm}(3900)$ state in the $\pi J/\psi$ invariant mass of the reaction $e^+e^- \to \pi^+\pi^- J/\psi$, with $J^P = 1^+$, mass $3881.2 \pm 4.2 \pm 52.7$ MeV, and width $51.8 \pm 4.6 \pm 36$ MeV. Signals for its neutral partner, $Z_c^0(3900)$, have also been found [27]. In the context of the present work, a natural question is the following: What is the impact of the reaction $J/\psi + \pi \to Z_c \to D + \bar{D}^*$ on the results found in the previous section? In order to estimate the influence of the $Z_c(3900)$ on such reactions, we consider the process of the absorption of J/ψ for a particular total electric charge, which can be 0, $+1$, or -1. The amplitude for this process can be written as

$$\mathcal{M}_Z = \alpha_{J/\psi\pi}\,\alpha_{D\bar{D}^*}\frac{1}{s - M_Z^2 + i M_Z \Gamma_Z} \times \left(-g^{\mu\nu} + \frac{p^\mu k'^\nu}{M_Z^2}\right)\epsilon^\mu(k)\epsilon^{\nu *}(p'), \tag{10}$$

where $M_Z = 3871.28$ MeV and $\Gamma_Z = 40$ MeV represent the mass and width of the $Z_c(3900)$ respectively. Also, $\alpha_{J/\psi\pi}$ and $\alpha_{D\bar{D}^*}$ are the couplings of the Z_c to the $J/\psi\pi$ and to the $D\bar{D}^*$ states, respectively, for a particular electric charge. To determine these couplings, we use the results of Ref. [28]. In Table I, we show the values found for these couplings for the channels of interest in this work. In the table, the quantities $\alpha_1 = 8128.3 - i\,53.0$ MeV and $\alpha_2 = 3300 - i\,923$ MeV represent the coupling of the Z_c to the states $\frac{1}{\sqrt{2}}(|D\bar{D}^*, I = 1\rangle + |D^*\bar{D}, I = 1\rangle)$ and $|J/\psi\pi\rangle$, which have isospin 1 and positive G parity. We follow the isospin phase convention $|\pi^+\rangle = -|1,1\rangle$, $|D^0\rangle = |D^{*0}\rangle = -|1/2, -1/2\rangle$.

The BESIII collaboration has also claimed the existence of an isospin 1 resonance, called $Z_c(4025)$ (width around

TABLE I. Couplings of the $Z_c(3900)$ found in Ref. [28] to the channels $J/\psi\pi$ and $D\bar{D}^*$ for different electric charges.

Channel	Coupling
$D^0\bar{D}^{*0}$, D^+D^{*-}	$-\alpha_1/2$, $\alpha_1/2$
$D^+\bar{D}^{*0}$, D^0D^{*-}	$\alpha_1/\sqrt{2}$, $-\alpha_1/\sqrt{2}$
$J/\psi\pi^0$, $J/\psi\pi^-$, $J/\psi\pi^+$	α_2, α_2, $-\alpha_2$

TABLE II. Coupling of the $Z_c(4025)$ found in Ref. [32] to the channels $J/\psi\rho$ and $D^*\bar{D}^*$ for different electric charges.

Channel	Coupling
$D^{*0}\bar{D}^{*0}$, $D^{*+}D^{*-}$	$-\eta_1/2$, $\eta_1/2$
$D^{*+}\bar{D}^{*0}$, $D^{*0}D^{*-}$	$\eta_1/\sqrt{2}$, $-\eta_1/\sqrt{2}$
$J/\psi\rho^0$, $J/\psi\rho^-$, $J/\psi\rho^+$	η_2, η_2, $-\eta_2$

25 MeV) in the $D^*\bar{D}^*$ invariant mass distribution of the reaction $e^+e^- \to \pi^\mp(D^*\bar{D}^*)^\pm$ [29]. Assuming that the $D^*\bar{D}^*$ pair interacts in the s wave, the authors of Ref. [29] have assigned to the $Z_c(4025)$ the quantum numbers $J^P = 1^+$. However, as stated by the same authors, the experiment cannot exclude other spin-parity assignments. In fact, as shown in Ref. [30], the invariant mass distribution found in Ref. [29] can be explained considering the $I^G(J^{PC}) = 1^-(2^{++})$ state with mass and width around 4000 and 90 MeV, respectively, which is generated as a consequence of the interaction of $D^*\bar{D}^* - \text{c.c.}$ and $J/\psi\rho$ in a coupled channel approach [31–33]. This interpretation is more plausible, since if the state $Z_c(4025)$ would have $J^P = 1^+$, as assumed in Ref. [29], it should have a large decay width to $J/\psi\pi$, as in case of the $Z_c(3900)$ mentioned above. However, in Refs. [25,29,34,35], no signal is found in the $J/\psi\pi$ invariant mass around 4025 MeV. Note that, theoretically, in both cases, the states $Z_c(3900)$ and $Z_c(4025)$ appear below the $D\bar{D}^*$ threshold for the former and below the $D^*\bar{D}^*$ threshold for the latter. However, as explained in Ref. [30], it is their corresponding widths that make possible their manifestation in the $D\bar{D}^*$ and $D^*\bar{D}^*$ invariant mass distribution found in Refs. [25,29,34,35].

As in the case of the $Z_c(3900)$, the exchange of $Z_c(4025)$ could also play an important role in the determination of the cross section of the reaction $J/\psi\rho \to D^*\bar{D}^*$ and its time-reversed process. In order to estimate this contribution, we consider the s-channel process $J/\psi + \rho \to Z_c(4025) \to D^* + \bar{D}^*$ and follow Ref. [32], where $Z_c(4025)$ is associated with the $I^G(J^{PC}) = 1^+(2^{++})$ state found at 3998 MeV with a width of 90 MeV in the T matrix obtained from the resolution of the Bethe-Salpeter equation considering $D^*\bar{D}^* - \text{c.c.}$, $J/\psi\rho$ as coupled channels. The amplitude associated with the process $J/\psi + \rho \to Z_c(4025) \to D^* + \bar{D}^*$ is given by

$$\mathcal{M}_{Z'} = \eta_{J/\psi\rho}\,\eta_{D^*\bar{D}^*}\frac{1}{s - M_{Z'}^2 + iM_{Z'}\Gamma_{Z'}} \times P^{\mu\nu\alpha\beta}(q)\epsilon_\mu(k)\epsilon_\nu(p)\epsilon^*_\alpha(k')\epsilon^*_\beta(p'), \quad (11)$$

where $M_{Z'} = 3989.61$ MeV and $\Gamma_{Z'} = 90$ MeV are, respectively, the mass and width found for the $Z_c(4025)$ in Ref. [32], $q = k + p = k' + p'$ is the total four-momentum, $\eta_{J/\psi\rho}$ and $\eta_{D^*\bar{D}^*}$ are the couplings of $Z_c(4025)$ to the channels $J/\psi\rho$ and $D^*\bar{D}^*$ for a particular total electric charge (0, +1, or −1), and $P^{\mu\nu\alpha\beta}(q)$ is the spin-2 projector, which is given by [33,36]

$$P^{\mu\nu\alpha\beta}(q) = \tfrac{1}{2}(\Delta^{\mu\alpha}\Delta^{\nu\beta} + \Delta^{\mu\beta}\Delta^{\nu\alpha}) - \tfrac{1}{3}\Delta^{\mu\nu}\Delta^{\alpha\beta}, \quad (12)$$

with

$$\Delta^{\mu\nu}(q) = -g^{\mu\nu} + \frac{q^\mu q^\nu}{M_{Z'}^2}, \quad (13)$$

and $g^{\mu\nu} = \text{diag}(1 - 1 - 1 - 1)$ is the metric tensor. The coupling constants $\eta_{J/\psi\rho}$ and $\eta_{D^*\bar{D}^*}$, as in the case of $Z_c(3900)$, can be calculated from the residue of the corresponding scattering matrix of Ref. [32] evaluated at the pole position. The value for these couplings are listed in Table II. In the table, the quantities $\eta_1 = 12560.80 - i\,507.80$ MeV and $\eta_2 = 8145.78 - i\,2627.96$ MeV represent the coupling of $Z_c(4025)$ to the states $\frac{1}{\sqrt{2}}(|D\bar{D}^*, I = 1\rangle - |D^*\bar{D}, I = 1\rangle)$ and $|J/\psi\rho\rangle$, which have isospin 1 and G parity negative. We follow the isospin phase convention $|\rho^+\rangle = -|1,1\rangle$, $|D^{*0}\rangle = -|1/2,-1/2\rangle$. With the above amplitudes, we can calculate the cross sections for J/ψ absorption and production in each one of the channels.

In Fig. 3, we show the cross sections of the processes $J/\psi + \pi \to D + \bar{D}^*$ and $J/\psi + \rho \to D + \bar{D}^*$ and the corresponding inverse processes. The solid lines show the results obtained in the previous subsections and the dashed lines show the effect of including the $Z_c(3900)$ and $Z_c(4025)$ as described above. As can be seen, the effect of the new resonances is small and will be neglected in what follows.

III. THERMALLY AVERAGED CROSS SECTIONS

We define the thermally averaged cross section for a given process $ab \to cd$ as [37–39]

$$\langle\sigma_{ab\to cd}\,v_{ab}\rangle = \frac{\int d^3\mathbf{p}_a\,d^3\mathbf{p}_b\,f_a(\mathbf{p}_a)\,f_b(\mathbf{p}_b)\,\sigma_{ab\to cd}\,v_{ab}}{\int d^3\mathbf{p}_a\,d^3\mathbf{p}_b\,f_a(\mathbf{p}_a)\,f_b(\mathbf{p}_b)}, \quad (14)$$

where v_{ab} represents the relative velocity of initial two interacting particles a and b and the function $f_i(\mathbf{p}_i)$ is the Bose-Einstein distribution (of particles of species i), which depends on the temperature T.

In the two upper panels of Fig. 4, we plot the thermally averaged cross sections for $\pi J/\psi$ absorption (on the left) and production (on the right) via the processes discussed in previous section. We can see that for all processes the production reactions are larger than the absorption ones. In the two lower panels of Fig. 4, we plot the thermally averaged cross sections for the $\rho J/\psi$ absorption and production. It can be noticed that they are comparable for all processes.

In the upper panels of Fig. 5, we plot the thermally averaged cross sections for the KJ/ψ absorption (on the left) and production (on the right). As before, the production reactions have larger cross sections than the corresponding inverse reactions. Finally, the thermally averaged cross sections for the K^*J/ψ absorption and production are plotted in the lower panels of Fig. 5. It can be seen that the J/ψ production cross sections are always larger than the respective absorption cross sections.

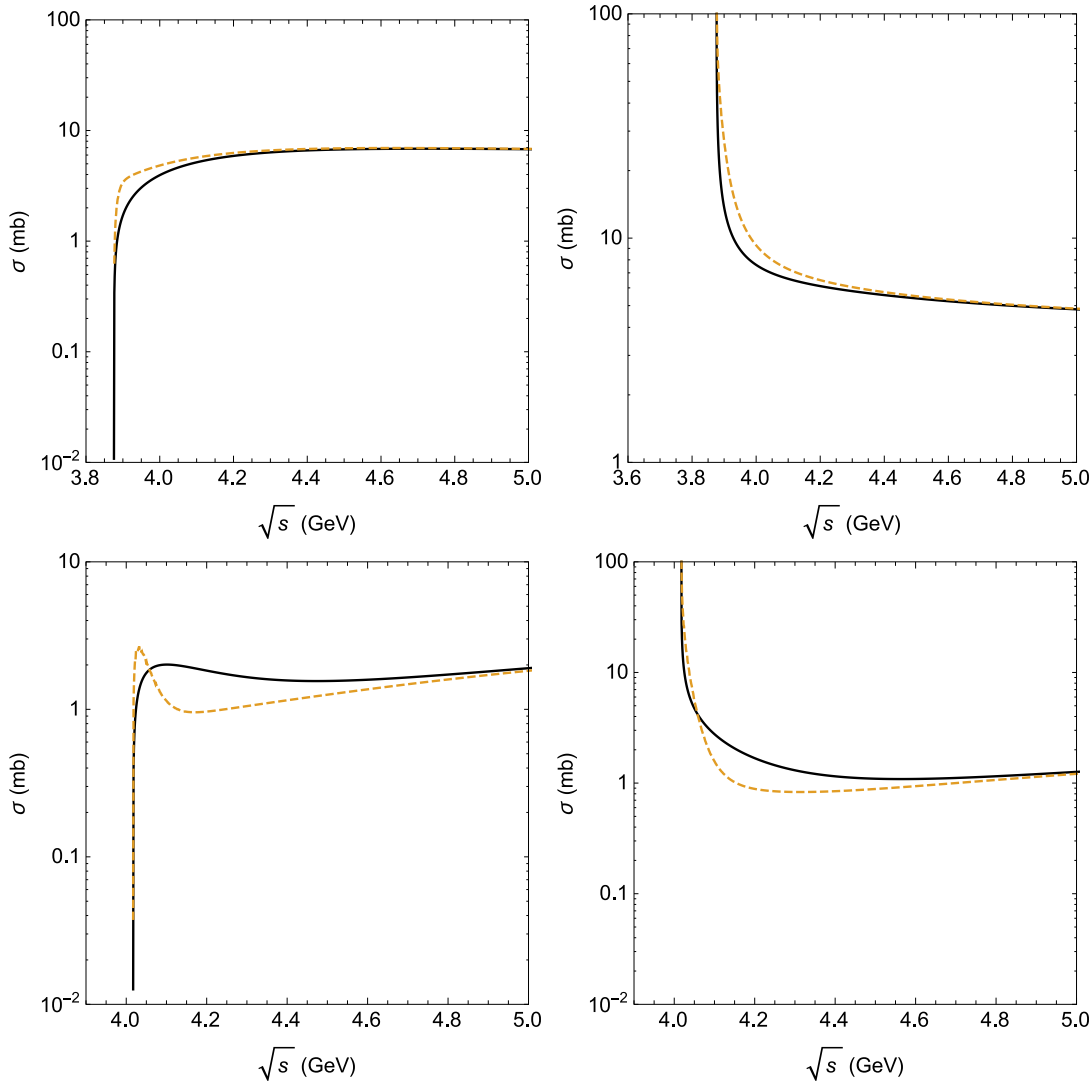

FIG. 3. J/Ψ absorption (top left) and production (top right) cross sections by π's. The solid lines represent the cross sections obtained without including the Z_c (3900) exchange in the s channel. The dashed lines show the results with the exchange of Z_c (3900) in the s channel included. Bottom panels show the J/Ψ absorption (bottom left) and production (bottom right) cross sections by ρ's. The solid lines in these panels show the cross sections obtained without including the Z_c (4025) exchange in the s channel. The dashed lines show the results obtained by including the $Z_c(4025)$ exchange in the s channel.

IV. TIME EVOLUTION OF THE J/ψ ABUNDANCE

We complete this study by addressing the time evolution of the J/ψ abundance in hadronic matter, using the thermally averaged cross sections estimated in the previous section. We shall make use of the evolution equation for the abundances of particles included in processes discussed above. The momentum-integrated evolution equation has the form [37–41]

$$\begin{aligned}\frac{dN_{J/\psi}(\tau)}{d\tau} = \sum_{\varphi=\pi,\rho K,K^*} & \Big[\big\langle\sigma_{D_{(s)}\bar{D}\to\varphi J/\psi} v_{D_{(s)}\bar{D}}\big\rangle n_{D_{(s)}}(\tau) N_{\bar{D}}(\tau) - \langle\sigma_{\varphi J/\psi\to D_{(s)}\bar{D}} v_{\varphi J/\psi}\rangle n_{\varphi}(\tau) N_{J/\psi}(\tau) \\ & + \big\langle\sigma_{D^*_{(s)}\bar{D}^*\to\varphi J/\psi} v_{D^*_{(s)}\bar{D}^*}\big\rangle n_{D^*_{(s)}}(\tau) N_{\bar{D}^*}(\tau) - \langle\sigma_{\varphi J/\psi\to D^*_{(s)}\bar{D}^*} v_{\varphi J/\psi}\rangle n_{\varphi}(\tau) N_{J/\psi}(\tau) \\ & + \big\langle\sigma_{D^*_{(s)}\bar{D}\to\varphi J/\psi} v_{D^*_{(s)}\bar{D}}\big\rangle n_{D^*_{(s)}}(\tau) N_{\bar{D}}(\tau) - \langle\sigma_{\varphi J/\psi\to D^*_{(s)}\bar{D}} v_{\varphi J/\psi}\rangle n_{\varphi}(\tau) N_{J/\psi}(\tau) \\ & + \big\langle\sigma_{D_{(s)}\bar{D}^*\to\varphi J/\psi} v_{D_{(s)}\bar{D}^*}\big\rangle n_{D_{(s)}}(\tau) N_{\bar{D}^*}(\tau) - \langle\sigma_{\varphi J/\psi\to D_{(s)}\bar{D}^*} v_{\varphi J/\psi}\rangle n_{\varphi}(\tau) N_{J/\psi}(\tau)\Big] \\ & + \sum_{\varphi=\bar{\pi},\bar{\rho},\bar{K},\bar{K}^*} \Big[\big\langle\sigma_{\bar{D}_{(s)}D\to\varphi J/\psi} v_{\bar{D}_{(s)}D}\big\rangle n_{\bar{D}_{(s)}}(\tau) N_{D}(\tau) - \langle\sigma_{\varphi J/\psi\to\bar{D}_{(s)}D} v_{\varphi J/\psi}\rangle n_{\varphi}(\tau) N_{J/\psi}(\tau)\end{aligned}$$

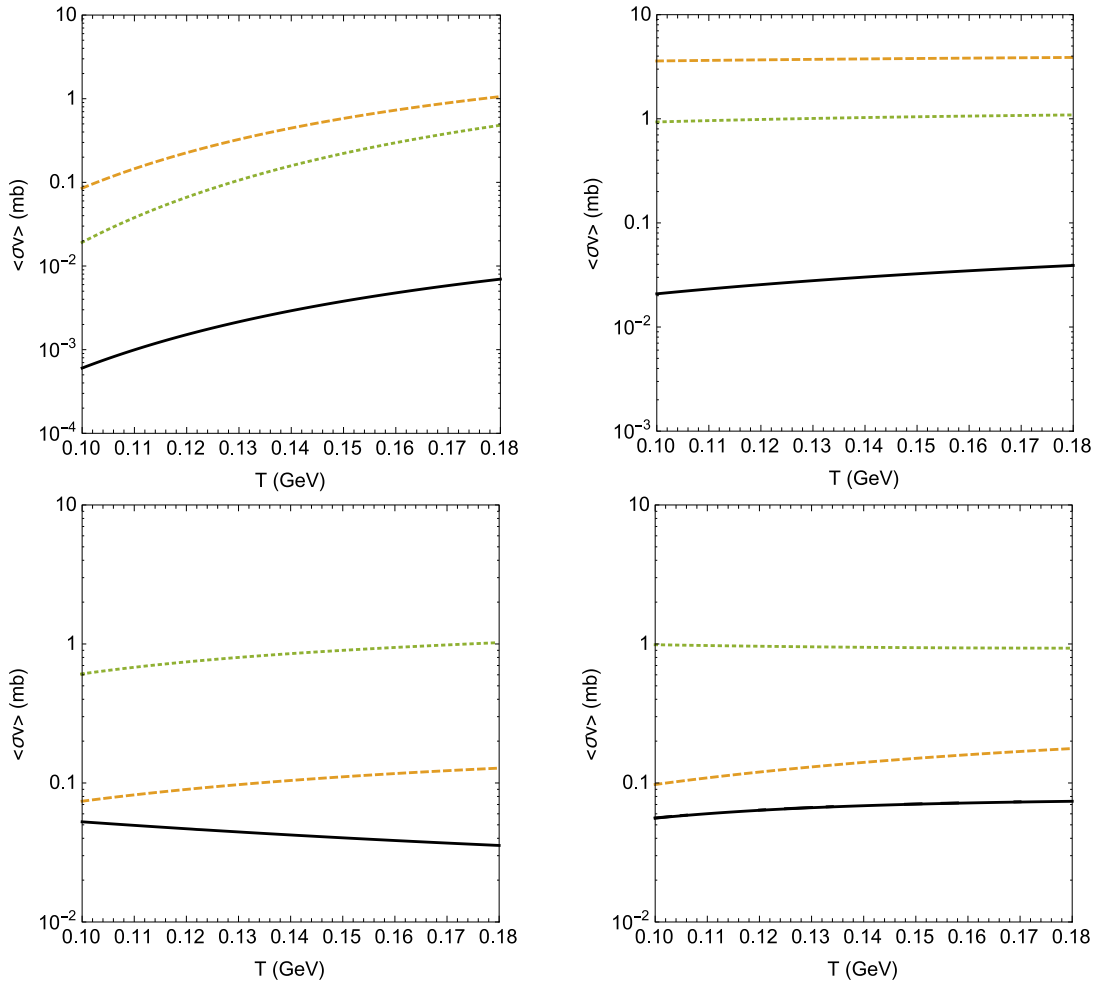

FIG. 4. J/Ψ absorption and production cross sections by π's and ρ's as a function of the temperature. Top left panel: absorption reactions with $\pi J/\Psi$ in the initial state. $\pi J/\Psi \to D\bar{D}$ (solid line), $\pi J/\Psi \to D^*\bar{D}$ (dashed lines), and $\pi J/\Psi \to D^*\bar{D}^*$ (dotted lines). Top right panel: production reactions with $\pi J/\Psi$ in the final state. The line convention is the same as in the left panel. Bottom left panel: absorption reactions with $\rho J/\Psi$ in the initial state. $\rho J/\Psi \to D\bar{D}$ (solid line), $\rho J/\Psi \to D^*\bar{D}$ (dashed line), and $\rho J/\Psi \to D^*\bar{D}^*$ (dotted line) Bottom right panel: production reactions with $\rho J/\Psi$ in the final state. The line convention is the same as in the left panel.

$$
\begin{aligned}
&+\left\langle\sigma_{\bar{D}^*_{(s)}D^*\to\varphi J/\psi}\, v_{\bar{D}^*_{(s)}D^*}\right\rangle n_{\bar{D}^*_{(s)}}(\tau)N_{D^*}(\tau) - \langle\sigma_{\varphi J/\psi\to\bar{D}^*_{(s)}D^*}\, v_{\varphi J/\psi}\rangle n_{\varphi}(\tau)N_{J/\psi}(\tau)\\
&+\left\langle\sigma_{\bar{D}^*_{(s)}D\to\varphi J/\psi}\, v_{\bar{D}^*_{(s)}D}\right\rangle n_{\bar{D}^*_{(s)}}(\tau)N_{D}(\tau) - \langle\sigma_{\varphi J/\psi\to\bar{D}^*_{(s)}D}\, v_{\varphi J/\psi}\rangle n_{\varphi}(\tau)N_{J/\psi}(\tau)\\
&+\left\langle\sigma_{\bar{D}_{(s)}D^*\to\varphi J/\psi}\, v_{\bar{D}_{(s)}D^*}\right\rangle n_{\bar{D}_{(s)}}(\tau)N_{D^*}(\tau) - \langle\sigma_{\varphi J/\psi\to\bar{D}_{(s)}D^*}\, v_{\varphi J/\psi}\rangle\Big],
\end{aligned}
\tag{15}
$$

where $n_\varphi(\tau)$ are $N_\varphi(\tau)$ denote the density and the abundances of π, ρ, K, K^*, charmed mesons and their antiparticles in hadronic matter at proper time τ. From Eq. (15), we observe that the J/ψ abundance at a proper time τ depends on the $\varphi J/\psi$ dissociation rate as well as on the $\varphi J/\psi$ production rate. We remark that in the rate equation we have also considered the processes involving the respective antiparticles, i.e., $\bar{\varphi} J/\psi \to \bar{D}^{(*)}_{(s)} D^{(*)}$ and $\bar{D}^{(*)}_{(s)} D^{(*)} \to \bar{\varphi} J/\psi$. However, these reactions have the same cross sections as the corresponding conjugate processes and the results reported above will be used to evaluate these contributions. We will assume that π, ρ, K, K^*, D, and D^* are in equilibrium. Therefore, the density $n_i(\tau)$ can be written as [37–41]

$$
n_i(\tau) \approx \frac{1}{2\pi^2}\gamma_i g_i m_i^2 T(\tau) K_2\left(\frac{m_i}{T(\tau)}\right), \tag{16}
$$

where γ_i and g_i are respectively the fugacity factor and the degeneracy factor of the relevant particle. The abundance $N_i(\tau)$ is obtained by multiplying the density $n_i(\tau)$ by the volume $V(\tau)$. The time dependence is introduced through the temperature $T(\tau)$ and volume $V(\tau)$ profiles appropriate to model the dynamics of relativistic heavy-ion collisions after the end of the quark-gluon plasma phase. The hydrodynamical expansion and cooling of the hadron gas is modeled as in Refs. [37–41] by

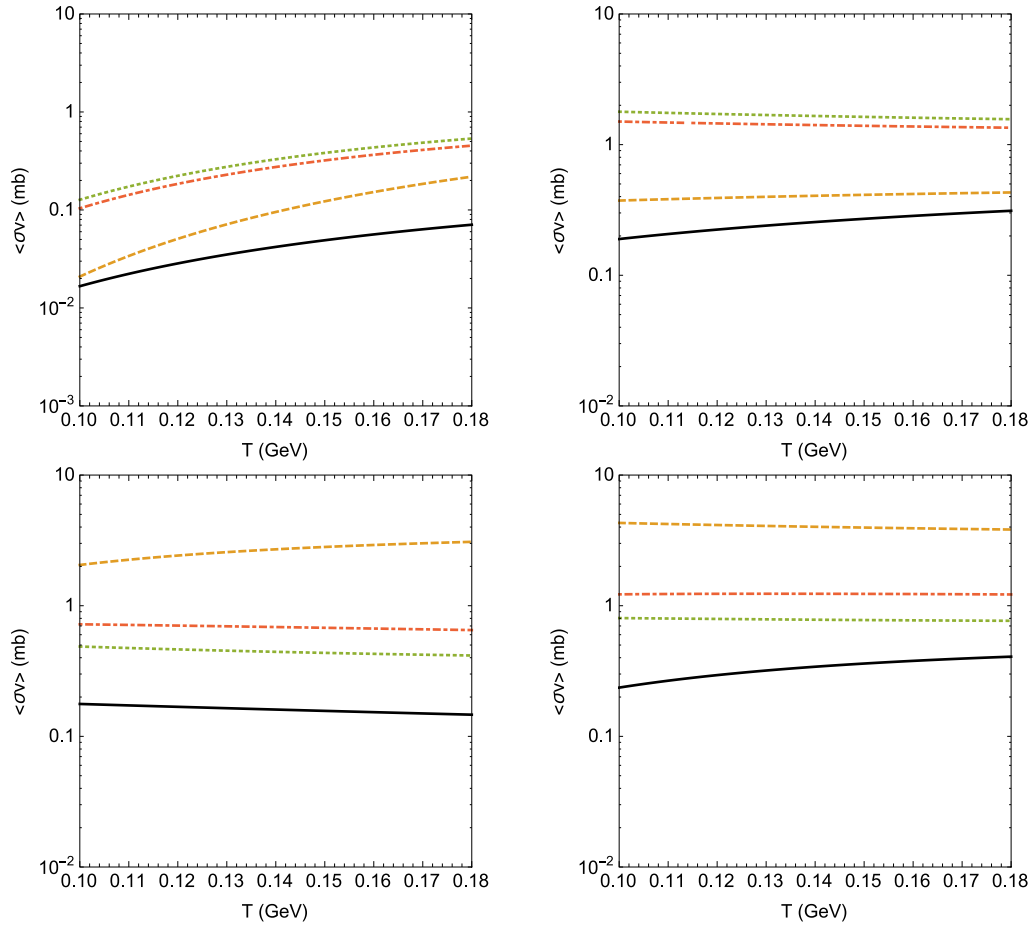

FIG. 5. J/ψ absorption and production cross sections by K's and K^*'s as a function of the temperature. Top left panel: absorption reactions with KJ/ψ in the initial state. $KJ/\psi \to D_s\bar{D}$ (solid line), $KJ/\psi \to D_s^*\bar{D}^*$ (dashed line), $KJ/\psi \to D_s^*\bar{D}$ (dotted line), and $KJ/\psi \to D_s\bar{D}^*$ (dot-dashed line). Top right panel: production reactions with KJ/ψ in the final state. The line convention is the same as in the left panel. Bottom left panel: absorption reactions with K^*J/ψ in the initial state. $K^*J/\psi \to D_s\bar{D}$ (solid line), $K^*J/\psi \to D_s^*\bar{D}^*$ (dashed line), $K^*J/\psi \to D_s^*\bar{D}$ (dotted line), and $K^*J/\psi \to D_s\bar{D}^*$ (dot-dashed line). Bottom right panel: production reactions with K^*J/ψ in the final state. The line convention is the same as in the left panel.

the boost-invariant Bjorken flow with an accelerated transverse expansion:

$$T(\tau) = T_C - (T_H - T_F)\left(\frac{\tau - \tau_H}{\tau_F - \tau_H}\right)^{\frac{4}{5}},$$

$$V(\tau) = \pi\left[R_C + v_C(\tau - \tau_C) + \frac{a_C}{2}(\tau - \tau_C)^2\right]^2 \tau_C. \quad (17)$$

In the equation above, R_C and τ_C fm/c denote the final transverse and longitudinal sizes of the quark-gluon plasma, while v_C and a_C are its transverse flow velocity and transverse acceleration at this time. $T_C = 175$ MeV is the critical temperature for the quark-gluon plasma to hadronic matter transition; $T_H = T_C = 175$ MeV is the temperature of the hadronic matter at the end of the mixed phase, occurring at the time τ_H. The freeze-out temperature $T_F = 125$ MeV then leads to a freeze-out time τ_F. In addition, we assume that the total number of charmed quarks in charmed hadrons is conserved during the processes. This number can be calculated with perturbative QCD and yields the charm quark fugacity factor γ_C in Eq. (16) [37–41]. The total number of pions and ρ mesons at freeze-out was taken from Refs. [39,42,43]. In the case of $K^{(*)}$ and $\bar{K}^{(*)}$ mesons [40], we work with the assumption that strangeness reaches approximate chemical equilibrium in heavy ion collisions due to the short equilibration time in the quark-gluon plasma and the net strangeness of the QGP is zero.

We will study the J/ψ evolution in the hadron gas formed in two types of collisions: central Au-Au collisions at $\sqrt{s_{NN}} = 200$ GeV at RHIC and central Pb-Pb collisions at $\sqrt{s_{NN}} = 5$ TeV at the LHC. The parameters which we need as input in Eqs. (17) are listed in Table 3.1 of Ref. [40] and, for convenience, are reproduced in Table III.

In Fig. 6, we present the time evolution of the J/ψ abundance as a function of the proper time for the two types of collisions discussed above: at RHIC (on the left panel) and at the LHC (on the right panel). Looking at the evolution equation, Eq. (15), we can see that the fate of the J/ψ population will be determined by the production and absorption cross sections and by the multiplicities of the other mesons, especially the pion multiplicity. While the cross sections alone would favor an enhancement of the J/ψ yield, the relative multiplicities favor its reduction, since in the hadron gas there are many more

TABLE III. Parameters used in the parametrization of the hydrodynamical expansion, given by Eqs. (17).

	$\sqrt{s_{NN}}$ (TeV)	v_C (c)	a_C (c^2/fm)	R_C (fm)	τ_C (fm/c)	τ_H (fm/c)	τ_F (fm/c)	γ_c	$N_{J/\psi}$
RHIC	0.2	0.4	0.02	8	5	7.5	17.3	6.4	0.017
LHC	5	0.6	0.044	13.11	5	7.5	20.7	15.8	1.67

pions and kaons (which hit and destroy the charmonium states) than D's, $\bar{D}$'s, D_s's, and $\bar{D}_s$'s (which can collide and create them). The result of this competition is a decrease of the J/ψ yield of approximately 20% at RHIC and 24% at the LHC. For comparison, we plotted the curves in the same time window. However, as can be seen in Table III, the system formed at the LHC lives longer as the J/ψ suppression is slightly larger. From the solid line in the figure, we can see that if there were only pions in the gas, there would be a small suppression of the J/ψ yield. This comes from a cancellation between a difference in the cross sections (the upper panels in Fig. 4) favoring production with a large difference in multiplicities, as pions are much more abundant than open charm mesons. The same competition occurs if the gas would include ρ's, kaons, and K^*'s.

In view of the uncertainties inherent to our calculations, all these numbers contain errors and should not be taken as definitive. A short list of the sources of uncertainties would certainly include the following items:

(i) The use of the SU(4) Lagrangian, which governs the interactions between particles. It could be replaced by some other theory. This would change the absolute values of the matrix elements of the reactions considered. We are primarily interested in the equilibruim (or absence of) between the absorption reactions and the corresponding productions reactions. A simple change in the magnitude of the matrix elements would not affect the final equilibrium, since they would be still connected by the same detailed balance relations. Increasing production will increase absorption in the same proportion.

(ii) The form factors. Both their functional form and the cutoff values could be changed. In fact, a small change in the cutoff parameters would already transform the lines in Fig. 6 into bands. However, as far as net changes in the J/ψ multiplicity are concerned, the same discussion of item (i) applies here.

(iii) The parametrization of the hydrodynamical expansion, Eqs. (17), could be changed by a more realistic one. This could make the system cool more quickly or slowly and consequently change the multiplicities of the different particles (π's, D's,...etc.) in different ways. This could potentially reverse the direction of the dynamics. For example, increasing the number of pions with respect to the number of open charm mesons would increase the absorption of J/ψ's.

In view of the above discussion, we conclude that even though there are still many aspects to be considered and/or improved, we believe that our main result, a moderate decrease of the number of J/ψ's throughout the hadron gas phase, is not likely to be dramatically changed. If confirmed, this result is very interesting for the physics of the quark gluon plasma, since J/ψ production will be mostly determined by the QGP dynamics.

V. CONCLUDING REMARKS

Precise measurements of J/ψ abundancies in heavy-ion collisions are an important source of information about the properties of the quark-gluon plasma phase. During this phase, J/ψ is produced by recombination of charm-anticharm pairs.

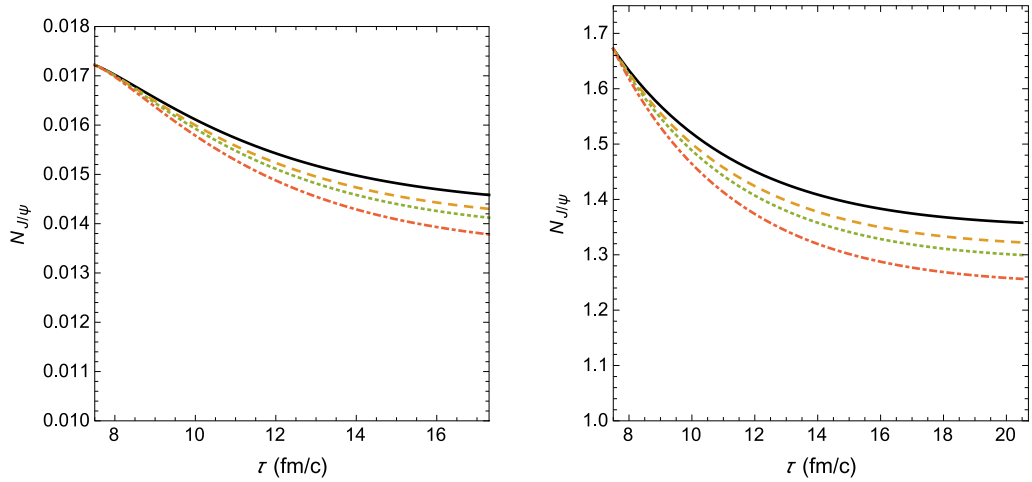

FIG. 6. Left: Time evolution of J/ψ abundance as a function of the proper time in central Au-Au collisions at $\sqrt{s_{NN}} = 200$ GeV. Solid, dashed, dotted, and dot-dashed lines represent the situations with only $\pi - J/\psi$ interactions and also adding the $\rho - J/\psi$, $K - J/\psi$, and $K^* - J/\psi$ contributions, respectively. Right: the same as on the left for LHC conditions.

However, after hadronization the J/ψ's interact with other hadrons in the expanding hadronic matter. Therefore, the J/ψ's can be destroyed in collisions with other comoving mesons, but they can also be produced through the inverse reactions. In order to evaluate the hadronic effects on the J/ψ abundance in heavy-ion collisions, one needs to know the J/ψ cross sections with other mesons.

In this work, we have studied J/ψ dissociation and production reactions, making use of effective field Lagrangians to obtain the cross sections for the processes $(\pi, \rho, K, K^*) + J/\psi \to D_{(s)}\bar{D}, D^{(*)}_{(s)}\bar{D}, D_{(s)}\bar{D}^{(*)}, D^*_{(s)}\bar{D}^*$ and the corresponding inverse processes. We have then computed the thermally averaged cross sections for the dissociation and production reactions, the latter being larger. Finally, we have used the thermally averaged cross sections as input in a rate equation and have followed the evolution of the J/ψ abundance in a hadron gas.

With respect to the existing calculations, the improvements introduced here are the inclusion of K and K^*'s in the effective Lagrangian approach (and the computation of the corresponding cross sections) and the inclusion of processes involving the new exotic charmonium states $Z_c(3900)$ and $Z_c(4025)$.

We conclude that the interactions between J/ψ and all the considered mesons reduce the original J/ψ abundance (determined at the end of the quark gluon plasma phase) by 20% and 24% in RHIC and LHC collisions respectively. Consequently, any really significant change in the J/ψ abundance comes from dissociation and regeneration processes in the QGP phase.

ACKNOWLEDGMENTS

We are deeply grateful to R. Rapp for reading our manuscript and making several enlightening observations. The authors would like to thank the Brazilian funding agencies CNPq (Contracts No. 310759/2016-1 and No. 311524/2016-8) and FAPESP (Contracts No. 12/50984-4 and No. 17/07278-5) for financial support.

[1] A. Mocsy, P. Petreczky, and M. Strickland, Int. J. Mod. Phys. A **28**, 1340012 (2013); R. Rapp, D. Blaschke, and P. Crochet, Prog. Part. Nucl. Phys. **65**, 209 (2010); P. Braun-Munzinger and J. Stachel, Landolt-Bornstein **23**, 424 (2010); L. Kluberg and H. Satz, *ibid.* **23**, 372 (2010), arXiv:0901.3831; R. Rapp and X. Du, Nucl. Phys. A **967**, 216 (2017); Phys. Rep. **621**, 76 (2016).

[2] A. Bourque and C. Gale, Phys. Rev. C **80**, 015204 (2009); **78**, 035206 (2008); A. Bourque, C. Gale, and K. L. Haglin, *ibid.* **70**, 055203 (2004); L. Maiani, F. Piccinini, A. D. Polosa, and V. Riquer, Nucl. Phys. A **741**, 273 (2004); Z. W. Lin and C. M. Ko, Phys. Rev. C **62**, 034903 (2000); J. Phys. G **27**, 617 (2001); F. S. Navarra, M. Nielsen, and M. R. Robilotta, Phys. Rev. C **64**, 021901(R) (2001).

[3] Y. Oh, T. Song, and S. H. Lee, Phys. Rev. C **63**, 034901 (2001); S. G. Matinyan and B. Müller, *ibid.* **58**, 2994 (1998).

[4] K. L. Haglin and C. Gale, Phys. Rev. C **63**, 065201 (2001); K. L. Haglin, *ibid.* **61**, 031902 (2000).

[5] F. Carvalho, F. O. Duraes, F. S. Navarra, and M. Nielsen, Phys. Rev. C **72**, 024902 (2005).

[6] J. P. Hilbert, N. Black, T. Barnes, and E. S. Swanson, Phys. Rev. C **75**, 064907 (2007); T. Barnes, E. S. Swanson, C.-Y. Wong, and X.-M. Xu, *ibid.* **68**, 014903 (2003); C. Y. Wong, E. S. Swanson, and T. Barnes, *ibid.* **62**, 045201 (2000); **65**, 014903 (2001); C.-Y. Wong, *ibid.* **65**, 034902 (2002); K. Martins, D. Blaschke, and E. Quack, *ibid.* **51**, 2723 (1995).

[7] F. O. Duraes, H. Kim, S. H. Lee, F. S. Navarra, and M. Nielsen, Phys. Rev. C **68**, 035208 (2003); F. O. Duraes, S. H. Lee, F. S. Navarra, and M. Nielsen, Phys. Lett. B **564**, 97 (2003); F. S. Navarra, M. Nielsen, R. S. Marques de Carvalho, and G. Krein, *ibid.* **529**, 87 (2002).

[8] E. G. Ferreiro, Phys. Lett. B **749**, 98 (2015); A. Capella, L. Bravina, E. G. Ferreiro, A. B. Kaidalov, K. Tywoniuk, and E. Zabrodin, Eur. Phys. J. C **58**, 437 (2008); T. Song and S. H. Lee, Phys. Rev. D **72**, 034002 (2005); P. Braun-Munzinger and K. Redlich, Eur. Phys. J. C **16**, 519 (2000).

[9] W. Cassing, L. A. Kondratyuk, G. I. Lykasov, and M. V. Rzjanin, Phys. Lett. B **513**, 1 (2001).

[10] O. Linnyk, E. L. Bratkovskaya, and W. Cassing, Int. J. Mod. Phys. E **17**, 1367 (2008).

[11] S. S. Adler *et al.* (PHENIX Collaboration), Phys. Rev. C **69**, 034909 (2004).

[12] B. Abelev *et al.* (ALICE Collaboration), Phys. Lett. B **736**, 196 (2014).

[13] R. S. Azevedo and M. Nielsen, Phys. Rev. C **69**, 035201 (2004); Braz. J. Phys. **34**, 272 (2004).

[14] R. S. Azevedo and M. Nielsen, arXiv:nucl-th/0407080.

[15] J. Schukraft, Nucl. Phys. A **967**, 1 (2017).

[16] A. Andronic *et al.*, Eur. Phys. J. C **76**, 107 (2016); S. Ganesh and M. Mishra, Nucl. Phys. A **947**, 38 (2016); E. Scomparin, Mod. Phys. Lett. A **28**, 1330018 (2013); L. Grandchamp and R. Rapp, Nucl. Phys. A **709**, 415 (2002).

[17] X. Du and R. Rapp, Nucl. Phys. A **943**, 147 (2015).

[18] For recent reviews, see F. K. Guo, C. Hanhart, U. G. Meißner, Q. Wang, Q. Zhao, and B. S. Zou, Rev. Mod. Phys. **90**, 015004 (2018); A. Hosaka, T. Iijima, K. Miyabayashi, Y. Sakai, and S. Yasui, PTEP **2016**, 062C01 (2016); M. Nielsen and F. S. Navarra, Mod. Phys. Lett. A **29**, 1430005 (2014).

[19] J. Zhou and X.-M. Xu, Phys. Rev. C **85**, 064904 (2012).

[20] S.-T. Ji, Z.-Y. Shen, and X.-M. Xu, J. Phys. G **42**, 095110 (2015).

[21] F.-R. Liu, S.-T. Ji, and X.-M. Xu, J. Korean Phys. Soc. **69**, 472 (2016).

[22] D. Gamermann, E. Oset, and B. S. Zou, Eur. Phys. J. A **41**, 85 (2009).

[23] We have identified two misprints in the expressions of some amplitudes $\mathcal{M}^{(K^*)}$ which appear in Ref. [14]: In the amplitude M_{2b}, third line in Eq. (22), the sign of the term $2p_4^\mu$ should be a minus sign; and in the amplitude M_{4d}, sixth line in Eq. (22), the $p_{4\rho}$ should be $p_{3\rho}$.

[24] F. Brazzi, B. Grinstein, F. Piccinini, A. D. Polosa, and C. Sabelli, Phys. Rev. D **84**, 014003 (2011).

[25] M. Ablikim *et al.* (BESIII Collaboration), Phys. Rev. Lett. **110**, 252001 (2013).
[26] M. Ablikim *et al.* (BESIII Collaboration), Phys. Rev. Lett. **112**, 022001 (2014).
[27] M. Ablikim *et al.* (BESIII Collaboration), Phys. Rev. Lett. **115**, 112003 (2015).
[28] F. Aceti, M. Bayar, E. Oset, A. M. Torres, K. P. Khemchandani, J. M. Dias, F. S. Navarra, and M. Nielsen, Phys. Rev. D **90**, 016003 (2014).
[29] M. Ablikim *et al.* (BESIII Collaboration), Phys. Rev. Lett. **112**, 132001 (2014).
[30] A. M. Torres, K. P. Khemchandani, F. S. Navarra, M. Nielsen, and E. Oset, Phys. Rev. D **89**, 014025 (2014).
[31] R. Molina and E. Oset, Phys. Rev. D **80**, 114013 (2009).
[32] F. Aceti, M. Bayar, J. M. Dias, and E. Oset, Eur. Phys. J. A **50**, 103 (2014).
[33] K. P. Khemchandani, A. M. Torres, M. Nielsen, and F. S. Navarra, Phys. Rev. D **89**, 014029 (2014).
[34] Z. Q. Liu *et al.* (Belle Collaboration), Phys. Rev. Lett. **110**, 252002 (2013).
[35] T. Xiao, S. Dobbs, A. Tomaradze, and K. K. Seth, Phys. Lett. B **727**, 366 (2013).
[36] A. Martinez Torres, K. P. Khemchandani, M. Nielsen, F. S. Navarra, and E. Oset, Phys. Rev. D **88**, 074033 (2013).
[37] S. Cho, T. Furumoto, T. Hyodo, D. Jido, C. M. Ko, S. H. Lee, M. Nielsen, A. Ohnishi, T. Sekihara, S. Yasui, and K. Yazaki (ExHIC Collaboration), Phys. Rev. Lett. **106**, 212001 (2011).
[38] S. Cho and S. H. Lee, Phys. Rev. C **97**, 034908 (2018).
[39] L. M. Abreu, K. P. Khemchandani, A. M. Torres, F. S. Navarra and M. Nielsen, Phys. Lett. B **761**, 303 (2016).
[40] S. Cho, T. Furumoto, T. Hyodo, D. Jido, C. M. Ko, S. H. Lee, M. Nielsen, A. Ohnishi, T. Sekihara, S. Yasui, and K. Yazaki (ExHIC Collaboration), Phys. Rev. C **84**, 064910 (2011).
[41] S. Cho *et al.* (ExHIC Collaboration), Prog. Part. Nucl. Phys. **95**, 279 (2017).
[42] L. W. Chen, C. M. Ko, W. Liu, and M. Nielsen, Phys. Rev. C **76**, 014906 (2007).
[43] S. Cho and S. H. Lee, Phys. Rev. C **88**, 054901 (2013).